STEM CELLS AND DEVELOPMENT
Volume 25, Number 24, 2016

DOI: 10.1089/scd.2016.0244

Effect of Secreted Molecules of Human Embryonic Stem Cell-Derived Mesenchymal Stem Cells on Acute Hepatic Failure Model

Majid Lotfinia,[1] Mehdi Kadivar,[1] Abbas Piryaei,[2,3] Behshad Pournasr,[2] Soroush Sardari,[4] Niloofar Sodeifi,[2] Forugh-Azam Sayahpour,[2] and Hossein Baharvand[2,5]

Adult tissue-derived mesenchymal stem cells (MSCs) show tremendous promise for a wide array of therapeutic applications predominantly through paracrine activity. Recent reports showed that human embryonic stem cell (ESC)-derived MSCs are an alternative for regenerative cellular therapy due to manufacturing large quantities of MSCs from a single donor. However, no study has been reported to uncover the secretome of human ESC-MSCs as treatment of an acute liver failure (ALF) mouse model. We demonstrated that human ESC-MSCs showed similar morphology and cell surface markers compared with bone marrow-derived MSCs. ESC-MSCs exhibited a higher growth rate during early in vitro expansion, along with adipogenic and osteogenic differentiation potential. Treatment with ESC-MSC-conditioned medium (CM) led to statistically significant enhancement of primary hepatocyte viability and increased immunomodulatory interleukin-10 secretion from lipopolysaccharide-induced human blood mononuclear cells. Analysis of the MSCs secretome by a protein array screen showed an association between higher frequencies of secretory proteins such as vascular endothelial growth factor (VEGF) and regulation of cell proliferation, cell migration, the development process, immune system process, and apoptosis. In this thioacetamide-induced mouse model of acute liver injury, we observed that systemic infusion of VEGF led to significant survival. These data have provided the first experimental evidence of the therapeutic potential of human ESC-MSC-derived molecules. These molecules show trophic support to hepatocytes, which potentially creates new avenues for the treatment of ALF, as an inflammatory condition.

Keywords: embryonic stem cells, mesenchymal stem cells, secretome, soluble factors, VEGF, acute liver failure

Introduction

Acute liver failure (ALF), the severe necrosis of hepatocytes, predominantly arises from viral hepatitis and drug-induced liver injury that leads to hepatic encephalopathy, coagulopathy, and progressive multiorgan failure [1]. Although definitive therapies for ALF do not exist, emergency liver transplantation is a relatively effective treatment option recommended for certain patients [2]. However, it is limited due to organ donor shortage, elevated costs, and the need for long-term use of immunosuppressive agents.

The introduction of stem cell therapy as treatment for liver diseases provides a promising approach for the future of liver regenerative medicine [3]. More than 500 registered clinical trials have been conducted using mesenchymal stem cells (MSCs) to treat degenerative and inflammatory disorders (http://clinicaltrials.gov), and liver diseases [4], primarily due to their capacity to suppress immune and inflammatory reactions as well as initiate normal tissue repair processes.

MSCs, nonhematopoietic, fibroblast-like, and multipotent stem cells can be isolated frequently from bone marrow (BM), adipose and placental tissues, and umbilical cord blood (for

[1]Biochemistry Department, Pasteur Institute of Iran, Tehran, Iran.
[2]Department of Stem Cells and Developmental Biology, Cell Science Research Center, Royan Institute for Stem Cell Biology and Technology, ACECR, Tehran, Iran.
[3]Department of Tissue Engineering, School of Advanced Technologies in Medicine, Shahid Beheshti University of Medical Sciences, Tehran, Iran.
[4]Drug Design and Bioinformatics Unit, Department of Medical Biotechnology, Biotechnology Research Center, Pasteur Institute of Iran, Tehran, Iran.
[5]Department of Developmental Biology, University of Science and Culture, Tehran, Iran.

review see Keating [5]). Studies have shown that transplantation of MSCs isolated from various tissues into ALF animal models have led to the suppression of liver destruction, supported resident hepatocyte functions, enhanced liver regeneration, and modulated inflammatory and immune reactions by paracrine secretions [6]. The exact mechanism by which MSCs exert their therapeutic effects is not fully understood. The secretion of a multitude of trophic factors with various properties may play a predominant role in the mechanisms of action to reduce tissue injury, protect tissue from further degradation, and/or enhance tissue repair [7]. Administration of MSC-conditioned medium (MSC-CM) has been shown to improve liver injury in preclinical studies [8,9]. However, limitations to harvesting MSCs from adult tissue include the availability of suitable donors, invasive procedures in most cases, limited number of cells obtained during the harvesting process, and restricted in vitro expansion capacity.

According to recent reports, MSCs could be derived from human embryonic stem cells (ESC-MSCs) with similar phenotypic characteristics such as multipotent differentiation potential, along with favorable immunomodulatory and anti-inflammatory properties that make them attractive candidates for regenerative cellular therapy [10]. To date, human ESC-MSCs have been used to treat various animal models such as inflammatory bowel disease [11], fistulizing Crohn's disease [12] and experimental autoimmune encephalitis [13]. However, no report has discussed the use of human ESC-MSC-CM in hepatocytes both in vitro and in an ALF mouse model.

We assessed the therapeutic potential of human ESC-MSC-CM by evaluating the viability and anti-inflammatory effects on mouse hepatocytes and mononuclear cells (MNCs) in vitro and on survival in an ALF model. We used antibody arrays in an attempt to profile the cytokines and growth factors to identify therapeutic candidates present in the CM. The results provided evidence that the therapeutic effects of ESC-MSC-CM were mostly attributed to vascular endothelial growth factor (VEGF).

Materials and Methods

Derivation of MSCs from human ESCs

Human ESC lines, RH6 and RH5 [14], were obtained from Royan Stem Cell Bank (Iran) and maintained in an undifferentiated state on mitomycin C (Sigma-Aldrich)-treated mouse embryonic fibroblasts. Cells were subcultured on Matrigel-coated plates (Sigma-Aldrich) in ESC medium that contained Dulbecco's modified Eagle's medium (DMEM)/F12 supplemented with 20% knockout serum replacement (KoSR); 2 mM L-glutamine, 0.1 mM nonessential amino acids (NEAAs), 1% insulin–transferrin–selenium (ITS) (all from Gibco); 0.1 mM β-mercaptoethanol (Sigma-Aldrich); and 5 μg/mL basic fibroblast growth factor (bFGF; Royan Biotech, Iran). The medium was renewed every other day and the cells were passaged every 5 days with collagenase IV (Sigma-Aldrich). We derived two human ESC-MSC lines from both ESC lines, according to a previously described protocol [15] with minor modifications. Human ESCs were trypsinized (Gibco), then nonadherently plated on Petri dishes at 2.5×10^5 cells/cm^2 and cultured in ESC medium plus 10 μM ROCK inhibitor Y-27632 (Calbiochem). After 2 days, we replaced the medium with a freshly prepared ESC medium without ROCK inhibitor. The cells were cultured for four more days to obtain ESC spheres. The spheres were maintained in ESC medium without bFGF for seven additional days until the formation of embryoid bodies (EBs). In this step, the medium was changed every 2 days. Subsequently, we transferred the EBs to 0.1% gelatinized plates. The EBs were maintained in MSC medium that consisted of low-glucose DMEM supplemented with 10% fetal bovine serum (FBS; Gibco) and 2 mM L-glutamine for 7–10 days. Then, the cells were replated and expanded for 1 week. In this step, the cells were defined as passage 0 (P0). At 80% confluency, the resultant cultures were passaged by trypsin/EDTA dissociation, counted, and seeded at a density of 1×10^4 cells/cm^2 in MSC medium. The medium was replaced every 2–3 days for 6 days. During cell expansion, we calculated the population doubling (PD) according to the cell numbers at the end of each passage (Nf) in relation to the cell numbers at the first passage (Ni), and according to the following formula: PD = log(Nf-Ni)/log 2. The cells were passaged every 6 days. The human BM-MSCs were obtained from Royan Stem Cell Bank and grown in the medium as previously described [16].

Multilineage differentiation of ESC-MSCs

For osteodifferentiation, MSCs (3×10^3 cells/cm^2) were cultured for 2 days in MSC medium, after which the medium was replaced by osteogenic medium that consisted of MSC medium supplemented with 50 μg/mL ascorbic acid, 10^{-7} M dexamethasone, and 10 mM β-glycerophosphate (all from Sigma-Aldrich). The medium was changed every 3 days. After 21 days, we assessed for osteodifferentiation by staining the cells with Alizarin Red.

For adipodifferentiation, we used the serum withdrawal/hypoxia (SW/H) method to differentiate ESC-MSCs into adipocytes, as described previously [17]. Briefly, MSCs were grown in ESC medium in 5% hypoxia conditions, and the medium was changed every 3 days for 14 days.

MSC-CM production

We cultured passage 4 human MSCs in a T150 culture flask that contained MSC medium until 80% confluency. After aspiration of the growth medium, cultures were washed three times with Dulbecco's phosphate-buffered saline (DPBS). Subsequently, we added 12 mL of DMEM medium supplemented with 0.05% human serum albumin and 2 mM L-glutamine to the cultures. The cultures were allowed to grow for a 24-h period. After collecting CM and removal of cell debris, the medium was concentrated to $\sim15\times$ by centrifugation at 4,000 *g* through a centrifugal ultrafilter unit that had a cut-off of <3 KD (Millipore). The concentrated CM was immediately cryopreserved at −80°C until use. The control medium [nonconditioned medium (NCM)] consisted of a similar medium without conditioning by human MSCs.

Primary hepatocyte culture

The hepatocytes were isolated from an adult mouse liver according to a previously reported two-step perfusion method with minor modifications [18]. Briefly, mice were anaesthetized using intraperitoneal (i.p.) injections of ketamine and xylazine at 100 and 10 mg/kg, respectively. After cannulation of the portal vein,

the liver was perfused with 25 mL of perfusion buffer that consisted of calcium-free Hank's balanced salt solution (1×, HBSS; Worthington), EGTA (0.5 mM; Sigma-Aldrich), and a penicillin/streptomycin solution (2%; Gibco). Next, the liver was perfused with 25 mL of dissociation solution that contained L15 medium, collagenase (50 U/mL; Worthington), and a penicillin/streptomycin solution (1%). Two perfusion steps were performed with a flow rate of 5 mL/min at 37°C. The perfused liver was excised from the mouse and placed in a dish that contained 25 mL of L15 medium. The cells were then released by cutting the liver with gentle shaking. The cell suspension was filtered using an 80 μm nylon mesh (BD Biosciences). To separate the parenchymal cells, we centrifuged the filtered suspension at 50 *g* for 2 min. Subsequently, the cell pellet was washed twice with Williams' Medium E. After the cells were counted, they were seeded at a density of 7.5×10^4 cells/cm^2 in Matrigel-coated plates that contained the attachment medium. The cells were allowed to incubate for 4 h at 37°C and 5% CO_2. The attachment medium consisted of Williams' Medium E (Gibco) supplemented with 20% FBS, 2 mM L-glutamine, and 2% penicillin/streptomycin solution. The medium was subsequently replaced with hepatocyte medium that contained HepatoZYME medium (Gibco) supplemented with 5% FBS, 2 mM L-glutamine, 0.1 mM NEAA, 1% ITS, and 1% penicillin/streptomycin solution. The hepatocyte medium was changed daily. After 48 h the cells were washed with DPBS, fixed in 4% paraformaldehyde, and incubated overnight with primary antibodies directed against mouse albumin at a temperature of 4°C. The cells were washed again, and then incubated for 1 h at 4°C with Alexa Fluor 488-conjugated secondary antibody. The cell nuclei were stained with 4, 6-diamidino-2-phenylindole (DAPI). Cell viability of hepatocytes treated with either CM or NCM was assessed by MTS (a tetrazolium compound) according to the manufacturer's protocol (Promega).

Immunomodulation assay

As previously described [19], 5 mL fresh blood was obtained from the donor and diluted in 5 mL DPBS. The diluted blood was gently poured onto a 5 mL Ficoll-Paque (GE Healthcare) and centrifuged at 1,500 *g* for 30 min. The buffy coat was collected and washed with DPBS. Subsequently, the cell pellet was resuspended in C10 medium that contained RPMI medium supplemented with 10% FBS, 2 mM L-glutamine, 0.1 mM NEAA, 0.1 mM β-mercaptoethanol, and penicillin/streptomycin. Primary human peripheral blood MNCs, at a density of 1×10^5, were seeded in a 96-well plate at 50 μL per well. After incubation for 30 min, we added either 50 μL of concentrated CM or NCM separately to each well. After 18 h, the cells were stimulated with 50 μL of lipopolysaccharide (LPS; final concentration: 10 μg/mL; Sigma-Aldrich) and incubated for 5 h. The supernatants were collected and ELISA was performed to assess for human interleukin-10 (IL-10) secreted from MNCs according to the manufacturer's instructions (Thermo Scientific).

Flow cytometry analysis and immunostaining

Human ESC-MSC and BM-MSC single-cell suspensions (passages 3, 4, and 5) were harvested using a 0.05% trypsin/EDTA solution. After FBS neutralization, the cells were washed twice with blocking buffer (1% FBS in DPBS), then incubated in blocking buffer for 30 min at 37°C. Next, 1×10^6 cells were separately incubated for 1 h at 4°C with an optimal dilution of conjugated monoclonal antibodies that included IgG1-PE (eBioscience), IgG1-FITC (eBioscience), anti-CD34-PE (BD Biosciences), anti-CD44-PE (eBioscience), anti-CD45-FITC (BD Biosciences), anti-CD73-PE (BD Biosciences), anti-CD90-FITC (Dako), and anti-CD105-PE (R&D Systems). Afterward, the cells were washed twice with DPBS, and then resuspended in DPBS. Flow cytometric experiments were performed with a BD FACSCalibur Flow Cytometer (BD Biosciences) and 10,000 events were acquired for each sample. Data were analyzed by the Flowing software.

For the immunofluorescence staining, the cells were allowed to incubate overnight in the presence of primary antibody against Alb (MAB1455; R&D Systems) at 4°C, and then we stained them with the appropriate Alexa Fluor-conjugated secondary antibody (A-11004; Invitrogen) at room temperature in the dark for 30 min. The cells were counterstained with DAPI (Sigma-Aldrich) for 5 min at room temperature and observed under a fluorescence microscope (IX71; Olympus).

RNA isolation and real-time reverse transcriptase polymerase chain reaction

Total RNA was extracted using TRI Reagent® (T9424; Sigma-Aldrich) from cells for quantitative reverse transcriptase polymerase chain reaction (RT-PCR) analysis as previously described [20]. cDNA was produced by the RevertAid First Strand cDNA Synthesis Kit (K1632; Fermantas) according to the manufacturer's instructions. Duplicate quantitative RT-PCR reactions were performed with the SYBR Green Master Mix (Ref 4367659; Applied Biosystems Life Technologies) with a real-time PCR system (Abi StepOnePlus; Applied Biosystems Life Technologies) and analyzed with StepOne software (version 2.1; Applied Biosystems Life Technologies). The samples were collected from either two or three independent biological replicates. The expression level of desired genes was normalized to *GAPDH*. Analysis was performed by the comparative CT method. Primers are listed in Supplementary Table S1 (Supplementary Data are available online at www.liebertpub.com/scd).

Antibody array

CM was prepared as described above. We performed semiqualitative assessment of 174 cytokines and growth factors with the RayBio Human Cytokine Antibody Array C2000 according to the manufacturer's instructions. The control was 15×CM. To detect chemiluminescence, the membranes were transferred to a Kodak imaging system. Densitometry data from the array images were extracted by NIH ImageJ software and analyzed by MeV software. Gene ontology (GO) Enrichment Analysis (geneontology.org) was used for GO analysis. The BioVenn application was used to draw the diagram.

ALF model

All animal experiments were carried out according to the NIH Guidelines for the Care and Use of Laboratory Animals after approval by the Royan Institute Ethics Committee.

Male inbred C57BL/6J mice were housed under standard conditions in a light-, temperature-, and humidity-controlled environment. ALF was induced in 8-week-old mice by

i.p. injections of 1,600 mg/kg thioacetamide dissolved in distilled water (Sigma-Aldrich). After 12 h, we randomly divided the mice into two groups. Mice in group 1 ($n=8$) received i.p. injections of 40 μg/kg recombinant VEGF (rVEGF; Royan BioTech, Iran) dissolved in DPBS, whereas group 2 ($n=6$) received DPBS as the vehicle. In another experiment, we randomly divided mice with liver injuries into four groups of eight mice per group, as follows: BM-MSC-CM (400 μL; group 1), RH6-MSC-CM (400 μL; group 2), and RH5-MSC-CM (400 μL; group 3). Group 4 received NCM as the control. For survival analysis, mice were monitored every day for up to 7 days and then euthanized through CO2 inhalation. In our experimental setting, mice died 12 h after thioacetamide administration (before CM treatments). Therefore, no unexpected deaths were observed during survival study.

For histopathological analyses, the liver tissue was fixed with 10% formalin, processed, and paraffin embedded. Serial sections (6 μm-thick) were stained with Hematoxylin and Eosin. Images were captured and we assessed the necroinflammatory score by the following parameters: piecemeal necrosis, confluent necrosis, focal lytic necrosis, apoptosis and focal inflammation, and portal inflammation according to a previous report [21]. Serum alanine aminotransferase (ALT) and aspartate aminotransferase (AST) enzyme activities were investigated using a commercial kit (Pars Azmun, Iran). For tissue and serum collection, three mice per group were euthanized through an i.p. injection of ketamine and xylazine at 48 h after treatments.

Statistical analysis

Data were expressed as mean ± standard deviation of the mean. Statistical significance was determined by ANOVA followed by Tukey. A $P<0.05$ was considered statistically significant.

Results

Derivation and characterization of human ESC-MSCs

MSCs were generated by isolation of outgrowing spontaneous differentiating cells from human ESCs. To derive ESC-MSCs, human ESC lines (RH6 and RH5) were nonadherently cultured in ESC medium for 4 days to form spheroids. Afterward, the spheroids were maintained in bFGF free-ESC medium for 1 week to obtain EBs. We generated ESC-MSCs by plating EBs on gelatin-coated plates in MSC growth medium. Outgrowing spontaneously differentiating cells were scraped at the edges of the plated EBs. They were further passaged to acquire a homogenous population that had spindle-shaped morphology and long extensions, which indicated an epithelial to mesenchymal transition over several passages (Fig. 1A).

Antigen profiling of the ESC-MSCs indicated highly expressed MSC markers CD44, CD73, CD90, and CD105, and the absence of hematopoietic surface markers CD34 and CD45 (Fig. 1B). ESC-MSCs were further characterized by their ability to undergo adipogenic and osteogenic differentiation (Fig. 1C, D). Adipogenic differentiation was confirmed by the accumulation of intracellular lipid droplets and validated by Oil Red staining and upregulation of adipocyte markers, *LPL* and *PPARγ*. Additionally, osteogenic differentiation yielded an extracellular precipitate, identified as calcium deposits by Alizarin Red staining, and upregulation of osteogenic markers, *RUNX* and *COL1*. Human ESC (RH6)-MSCs showed a higher proliferation rate than BM-MSCs. Additionally, hESC (RH5)-MSCs showed a stable expansion while the expansion ability of BM-MSCs was diminished after four passages (Fig. 1E).

Factors secreted by MSCs protected hepatocyte viability and showed immunomodulatory effect in vitro

We studied the trophic effects of MSC-CM on the mouse liver. In this research, mouse primary hepatocytes were isolated by two-step perfusion, then cultured in hepatocyte medium for 24 h (Fig. 2A). The cultured cells exhibited epithelial morphology with prominent nuclei. ALB stained positive with fluorescent-conjugated antibody (Fig. 2B). After 24 h, the primary hepatocytes were treated with 15× concentrated CM (50% CM and 50% Williams' medium), and cell viability was quantified after 48 h. MTS analysis showed that CM derived from BM-MSCs and ESC-MSCs (RH6-MSCs and RH5-MSCs) increased cell viability compared

FIG. 1. Generation and characterization of human ESC-MSCs. **(A)** The protocol for differentiation of human ESC (RH6 and RH5 lines) into MSCs. The detailed differentiation procedure is explained in the Materials and Methods section. Sequential morphological changes of epithelial ESCs into mesenchymal cells during differentiation are shown by inverted phase contrast microscope. **(B)** Immunophenotyping of RH6-MSCs, RH5-MSCs, and human bone marrow MSCs (BM-MSCs). The three cell types (passages 3–5) are examined by flow cytometry. Analysis of MSC markers, including CD44, CD73, CD90, and CD105, as well as hematopoietic markers CD34 and CD45 (double staining by anti-CD34-PE and anti-CD45-FITC) was performed by Flowing software (version 2.5.1). The white histogram represents the cells stained with isotype control antibodies. Expression of CD markers is presented as the mean ± SD of three different passages. **(C)** In vitro differentiation of MSCs into mesodermal lineages (adipocytes and osteoblasts). Adipodifferentiation was performed by the serum withdrawal/hypoxia method. Lipid droplets in cells stained with Oil Red O (*upper panel*) after 2 weeks. For osteodifferentiation of MSCs, we cultured the cells in osteogenic media for 3 weeks. Alizarin Red staining showed deposits of calcium crystals (*lower panel*). Scale bars: 100 μm. **(D)** The in vitro differentiation potential of MSCs (BM-MSC and RH6-MSC) was confirmed by studying the expressions of *LPL* and *PPARG* for adipodifferentiation and *RUNX* and *COL1* for osteodifferentiation by real-time RT-PCR. BM-MSCs and ESC-MSCs after differentiation were compared with control groups (MSCs cultured in nondifferentiated medium). **(E)** Growth characteristics of ESC-MSCs. Graph shows PD over time (6 passages) for three different human cells -BM-MSCs, RH6-MSCs, and RH5-MSCs. During cell expansion, PD was calculated based on the cell numbers at the end of every passage in relation to the cell numbers at the first passage. BM, bone marrow; ESC, embryonic stem cell; MSCs, mesenchymal stem cells; PD, population doubling; RT-PCR, reverse transcriptase-polymerase chain reaction; SD, standard deviation. Color images available online at www.liebertpub.com/scd

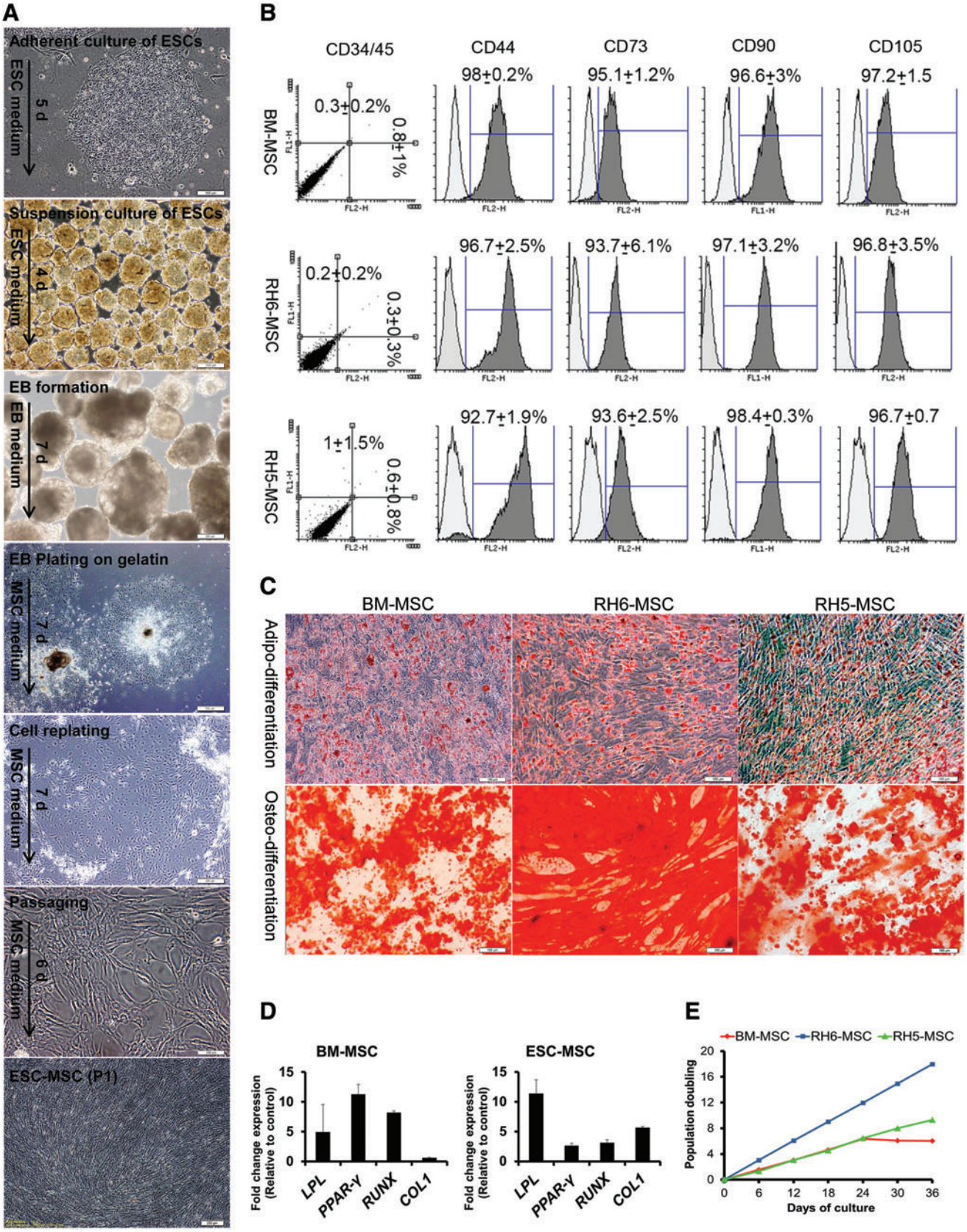
A
Adherent culture of ESCs
ESC medium
5 d
Suspension culture of ESCs
ESC medium
4 d
EB formation
EB medium
7 d
EB Plating on gelatin
MSC medium
7 d
Cell replating
MSC medium
7 d
Passaging
MSC medium
6 d
ESC-MSC (P1)
B
CD34/45
CD44
CD73
CD90
CD105
BM-MSC
0.3±0.2%
0.8±1%
98±0.2%
95.1±1.2%
96.6±3%
97.2±1.5
RH6-MSC
0.2±0.2%
0.3±0.3%
96.7±2.5%
93.7±6.1%
97.1±3.2%
96.8±3.5%
RH5-MSC
1±1.5%
0.6±0.8%
92.7±1.9%
93.6±2.5%
98.4±0.3%
96.7±0.7
C
BM-MSC
RH6-MSC
RH5-MSC
Adipo-differentiation
Osteo-differentiation
D
BM-MSC
ESC-MSC
Fold change expression (Relative to control)
LPL
PPAR-γ
RUNX
COL1
E
BM-MSC
RH6-MSC
RH5-MSC
Population doubling
Days of culture

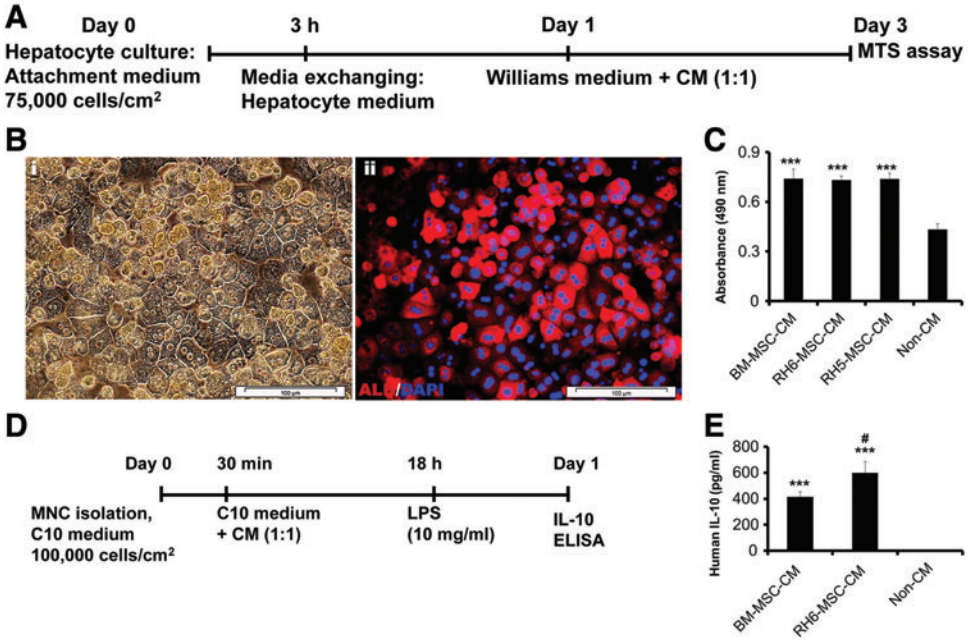

FIG. 2. In vitro effects of human ESC-MSC-CM and BM-MSC-CM on hepatocyte viability and MNC immunomodulation. **(A)** Schematic diagram of the experimental procedure to study the trophic potential of MSC-CM on mouse primary hepatocytes. Two-step collagenase perfusion was used for mouse hepatocyte isolation. Isolated cells were initially cultured on plates that contained Williams' medium for 3 h, after which the medium was replaced by hepatocyte medium (HepatoZYME + supplements) for 1 day and then incubated in Williams' medium + CMs for 2 days. **(B)** Immunostaining for ALB. **(i)** Cultured hepatocytes represented epithelial morphology and formed a stable monolayer such as polygonal cells with one or two round, prominent nuclei. **(ii)** Albumin-expressing hepatocytes visualized by immunostaining and fluorescent microscopy. Nuclei stained with DAPI. Scale bar: 100 μm. **(C)** We used the MTS assay to assess for primary cultured hepatocyte viability in the presence of MSC-CM or NCM. Human BM-MSC-CM and human ESC-derived MSC-CM (RH6-MSC-CM and RH5-MSC-CM) increased hepatocyte survival compared with NCM. **(D)** Schematic diagram of an in vitro immunomodulation assay. Primary human peripheral blood MNCs were first incubated in the presence of MSC-CM and NCM for 18 h, then stimulated with LPS for 5 h. Finally, we measured the level of IL-10 secreted from MNCs as an indicator for anti-inflammatory activity. **(E)** ELISA was used to assess the level of IL-10 in MNC culture supernatant. Incubation of MNCs with MSC-CM led to increased secretion of IL-10 from MNCs. Results have been reported as a mean of experiments performed in triplicate. $^{***}P < 0.001$ for MSC-CM compared with NCM. $^{\#}P < 0.05$ for ESC-MSC-CM compared with BM-MSC-CM. CM, conditioned medium; DAPI, 4, 6-diamidino-2-phenylindole; IL-10, interleukin-10; LPS, lipopolysaccharide; MNCs, mononuclear cells; NCM, nonconditioned medium. Color images available online at www.liebertpub.com/scd

with NCM (Fig. 2C, $P < 0.001$), but there was no significant difference between different CMs.

We evaluated the effects of ESC-MSC-CM on the increase in IL-10 secretion from LPS-induced MNCs as an indicator of immunomodulation by ELISA (Fig. 2D). Incubation of MNCs with BM-MSC-CM and ESC-MSC-CM led to increased secretion of IL-10 from MNCs compared with NCM (Fig. 2E, $P < 0.001$). There was increased IL-10 secretion from ESC-MSC-CM-treated MNCs compared with BM-MSC-CM-treated MNCs (Fig. 2E, $P < 0.05$).

Therefore, secreted proteins from BM-MSCs and ESC-MSCs had significant trophic effects on hepatocyte viability. The immunomodulatory potential of ESC-MSCs was more than BM-MSCs as indicated by increased IL-10 secretion.

MSC-CM effects on the in vivo ALF model

To evaluate the therapeutic potential of BM-MSC-CM and ESC-MSC-CM for liver regeneration, after 12 h, we injected 15× concentrated CMs into the peritoneal cavities of thioacetamide-induced mouse models of ALF (Fig. 3A). At 48 h after injection of BM-MSC-CM and ESC-MSC-CM, the levels of hepatic enzymes (AST and ALT) significantly decreased compared with non-CM (Fig. 3B). Additionally, histopathological analysis showed that ALF mice treated with BM-MSC-CM and RH6-MSC-CM decreased the necroinflammatory score (Fig. 3C, D). However, we observed no survival benefit after 1 week in animals treated with BM-MSC-CM and ESC-MSC-CM (Fig. 3E).

Profiling of BM-MSC and ESC-MSC secretomes

In an effort to determine which secretory proteins had trophic and immunomodulatory effects, we profiled BM-MSC-CM and ESC-MSC-CM using an antibody array. Although both samples contained a majority of assessed cytokines and growth factors, BM-MSCs, when compared with ESC-MSCs, generally expressed a higher level of secretory proteins (Fig. 4A). A comparison of secretory proteins between BM-MSCs and ESC-MSCs showed that 4 proteins upregulated in ESC-MSCs—angiogenin, IGFBP2, TGFβ1, and MCP1 (Fig. 4B). Quantity analysis of the ESC-MSC secretome indicated that 35 proteins expressed at higher levels than the others (Fig. 4C). We analyzed the distribution of these 35 proteins in GO categories to

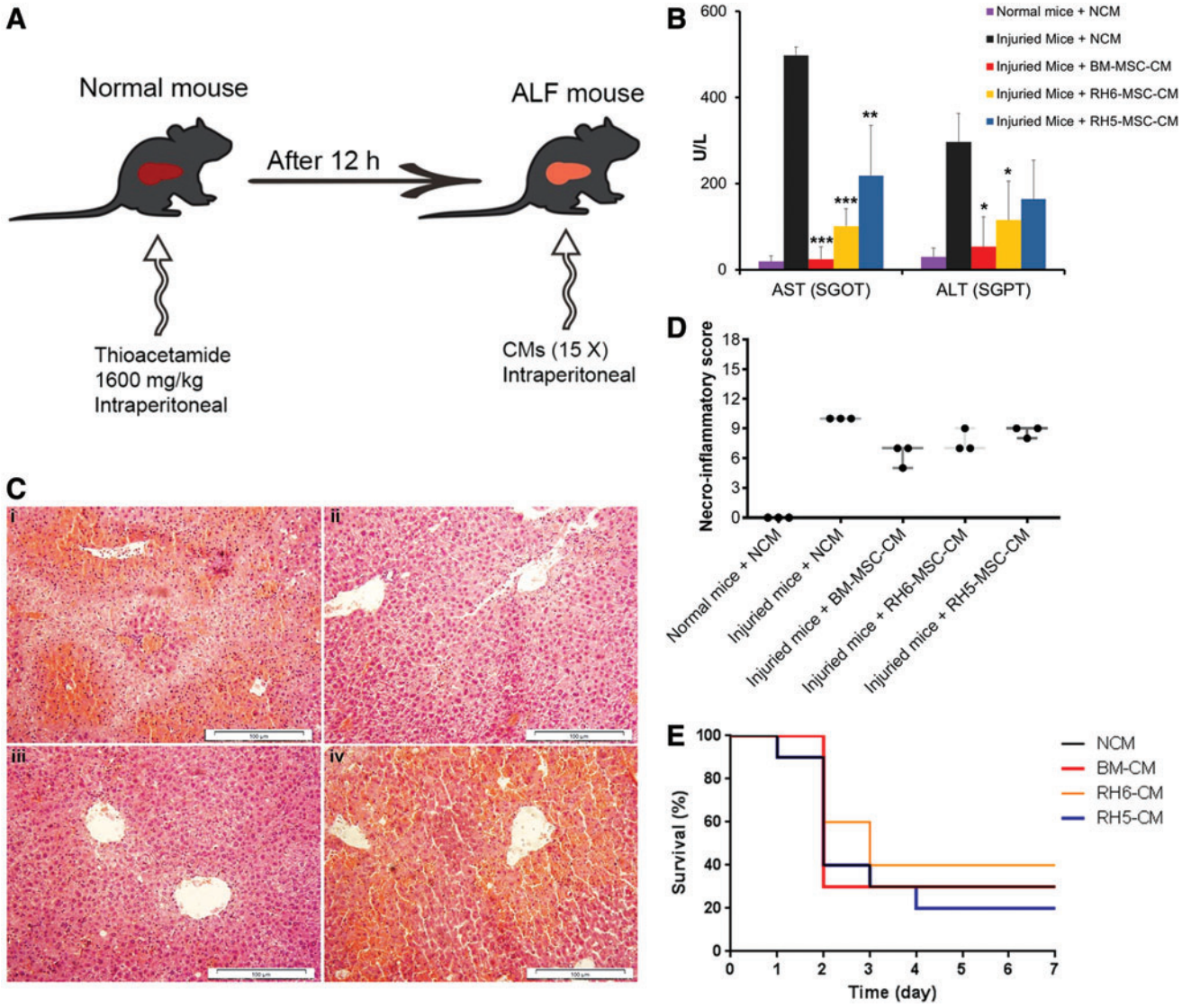

FIG. 3. In vivo effects of human SCs and their CM on mice with ALF. **(A)** Schematic representation of the experimental procedure design. **(B)** Biochemical assessment of AST and ALT in blood serum of ALF mice treated with human MSC-CM ($n=3$) after 48 h. Data were reported as mean ± SD. $*P<0.05$, $**P<0.01$, and $***P<0.001$. **(C)** Representative micrographs of liver tissue. Liver sections from various groups stained with Hematoxylin and Eosin. Injured mice treated with **(i)** NCM, **(ii)** BM-MSC-CM, **(iii)** RH6-MSC-CM, and **(iv)** RH5-MSC-CM. Scale bar: 100 µm. **(D)** Histopathological grading of necrosis and inflammation of the liver ($n=3$). Liver injury induced by injection of thioacetamide led to necrosis and inflammation. Treatment with MSC-CMs, unlike NCM, decreased the necroinflammatory score. Each circle represents one mouse. **(E)** Survival rate of ALF mice treated with CM. After 12 h, 400 µL of 15 × concentrated CM from RH6-MSCs, RH5-MSCs, and BM-MSCs were injected intraperitoneally (i.p.) into thioacetamide-mediated ALF mice ($n=10$ per group). NCM was used as the control. ALF, acute liver failure; ALT, alanine aminotransferase; AST, aspartate aminotransferase; Color images available online at www.liebertpub.com/scd

investigate the experimental biological processes in which they were involved. Significantly, higher frequencies of secretory proteins were associated with regulation of cell proliferation, cell migration, the development process, immune system process, and apoptosis (Fig. 4D). Interestingly, further analysis showed that ESC-MSCs expressed proteins that included BMP4 and VEGF, which regulated epithelial cell proliferation, the immune system, and apoptosis (Fig. 4D).

In light of the therapeutic role of VEGF on hepatic failure, we evaluated its role in the ALF mouse model. For this purpose, ALF mice received i.p. injections of rVEGF after 12 h. We evaluated their survival rate. The results indicated that the percentage survival rates of mice that received rVEGF was ∼66% compared with ∼33% in the vehicle group (Fig. 4E).

Discussion

In this study we differentiated human ESCs into MSC-like cells. The resultant MSCs showed that over 90% of the cells were positive for CD44, CD73, CD90, and CD105, whereas negative for hematopoietic markers, CD34, CD45.

These MSCs had the ability to differentiate into osteoblasts and adipocytes. Consistent with Olivier et al. [17] results, we showed that the SW/H method was a highly efficient approach for the induction of adipodifferentiation. Human ESC-MSCs exhibited a higher proliferation rate and longer expansion than BM-MSCs, which agreed with other studies [22]. Of note, the MSC proliferation rates depended on their developmental age, such that adult-derived MSCs proliferated slowly in culture, whereas fetal-derived MSCs proliferated at a faster rate. Due to ESC-MSC rapid rate of proliferation, they showed greater potential for scale-up expansion for therapeutic purposes.

Primary hepatocytes and LPS-induced MNCs were treated by ESC-MSC-CMs. ESC-MSC increased hepatocyte viability in vitro and also resulted in higher secretion of IL-10 as an anti-inflammatory cytokine from MNCs compared with BM-MSCs in vitro. Consistent with our study, a number of reports demonstrated that BM-MSC secretory molecules had the ability to decrease apoptotic hepatocellular death and increase hepatocyte proliferation [8]. In addition, it was shown that BM-MSC secretory molecules had the capability to induce IL-10 secretion from MNCs as an anti-inflammatory marker [23]. Therefore, it could be deduced that ESC-MSCs had trophic and anti-inflammatory effects on the in vitro model.

To assess the therapeutic effects of BM-MSCs and ESC-MSCs in vivo, the concentrated CM from these cells were injected individually into mice that had thioacetamide-induced liver failure. Although BM-MSC-CM and ESC-MSC-CM improved the biochemical and histopathological parameters of the injured livers, they failed to improve the survival rate of these mice. However, Parekkadan et al. reported that BM-MSC-CM could provide a significant survival benefit in rats with D-galactosamine-induced liver failure [9]. Although this might be related to the heterogeneity of ESC-MSCs or animal models in both studies, we could not clearly explain why ESC-MSC-CM did not cause recovery in the liver-injured mice in the current study.

To determine the presence of trophic and immunomodulatory secretes, we analyzed the ESC-MSC and BM-MSC secretomes according to the cytokine array. The results revealed that BM-MSCs were a rich source of cytokines compared with ESC-MSCs. However, the in vitro study demonstrated that ESC-MSCs exhibited more potent anti-inflammatory properties than BM-MSCs, which could be attributed to the presence of highly expressed mediators in ESC-MSCs that included angiogenin, IGFBP2, TGF-β1, and MCP1, which have been shown to reduce inflammation [24] or have a pivotal role in positive regulation of the immune system [25]. It was demonstrated that ESC-MSCs inhibited CD83 upregulation and IL-12p70 secretion from dendritic cells and enhanced regulatory T cell populations induced by interleukin 2 (IL-2) [22]. Additionally, ESC-MSCs and induced pluripotent stem cell-derived MSCs (iPSC-MSCs) had similar immunogenic properties, but more potent immunomodulatory effects compared with BM-MSCs [22]. Among the molecules secreted from ESC-MSCs, we determined that 35 factors had higher expressions. More importantly, BMP4 and VEGF molecules were associated with biological processes such as regulation of epithelial cell proliferation and the immune system process, as well as negative regulation of the apoptotic process. Recent studies showed that BMP4 was a paracrine inhibitor of liver regeneration [26–28]. VEGF, a trophic factor, has emerged as an important mediator of immune tolerance in the tumor microenvironment [29]. Therefore, we focused on the therapeutic roles of VEGF in ALF. Our results revealed that the survival rate of rVEGF-administered mice was two times greater than vehicle-treated mice. CM showed improved biochemical and histopathological parameters, but failed to improve mouse survival rates; however, rVEGF could ameliorate the survival rate. This may relate to higher concentration of injected rVEGF (2 μg) compared with lower one in CM (<50 ng) [30]. In a study by Parekkadan et al., it was determined that treatment with BM-MSC-CM altered immune cell migration to the liver. In another study, they revealed that chemokines present in BM-MSC-CM played a vital role for the treatment of ALF in models [9]. Banas et al. suggested that the ability of adipose tissue-derived MSCs to treat ALF models was presumably attributed to several secretory molecules—IL-1R, IL-6, IL-8, G-CSF, GM-CSF, MCP1, NGF, and HGF [31]. Additionally, it has been indicated that liver recovery might be induced through anti-inflammatory mediators such as interleukins IL-10, IL-1ra, IL-13, and IL-27 in hepatic progenitor CM. Blocking studies of IL-10 secretion from these cells confirmed the therapeutic potential of this cytokine in ALF mouse models [32].

FIG. 4. Secretory profiling of human ESC-MSCs and BM-MSCs. **(A)** Heat map of cytokine secretion. The cytokine array (C2000; RayBio) was used to interrogate various cytokines and growth factors in human RH6-MSC and BM-MSC-CM. We assayed 174 secreted molecules (60 molecules for array C6, 60 for C7, and 54 for C8) in BM-MSC-CM and ESC-MSC-CM. These assays were performed in duplicate. Protein signals were quantified by NIH ImageJ software and normalized to the signal intensity average of positive controls for each array. Heat maps were generated by MeV software. From left to right: heat map of array C6, C7, and C8. Quantification of the samples revealed that the concentration of most cytokines in BM-MSC-CM was greater than ESC-MSC-CM. **(B)** Secretory proteins (4 proteins) showed greater expression in ESC-MSCs compared with BM-MSCs (fold change: >1.2). **(C)** List of 35 secretory proteins present at high levels (normalized signal intensity >0.5) in RH6-MSC-CM. **(D)** GO analysis of 35 selected cytokines and growth factors from ESC-MSC-CM. These ESC-MSC secretory proteins were analyzed by GO Enrichment Analysis Tools. The graph has indicated a number of biological processes (experimental) in which the 35 selected proteins are involved ($P < 0.05$). Venn diagram shows overlap between three biological processes—regulation of immune response (*red circle*), epithelial cell proliferation (*green circle*), and negative regulation of apoptosis (*blue circle*). A total of 16 out of 35 proteins were related to these three biological processes, VEGF and BMP4 of which are common in these biological processes. **(E)** Survival rate of ALF mice treated with rVEGF. Mice in group 1 ($n = 8$) received i.p. injection of 40 μg/kg rVEGF dissolved in DPBS. Group 2 ($n = 6$) received DPBS as the vehicle. DPBS, Dulbecco's phosphate-buffered saline; GO, gene ontology; rVEGF, recombinant VEGF; VEGF, vascular endothelial growth factor. Color images available online at www.liebertpub.com/scd

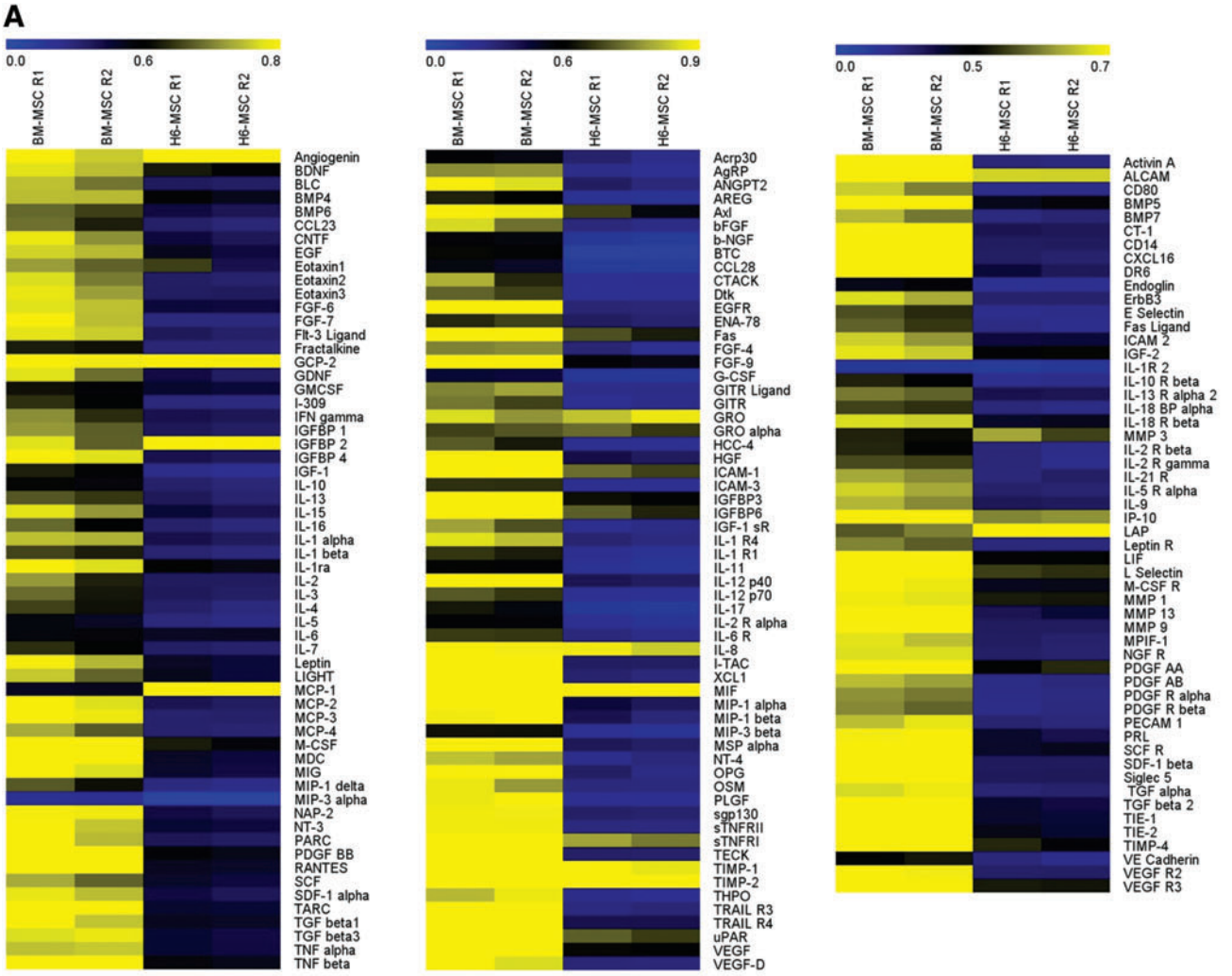

B

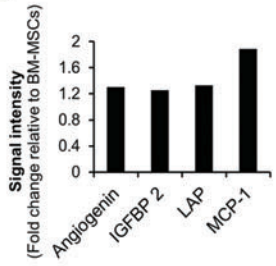

C

Protein Name	Uniprot Accession Number	Protein Name	Uniprot Accession Number	Protein Name	Uniprot Accession Number	Protein Name	Uniprot Accession Number	Protein Name	Uniprot Accession Number
Angiogenin	P03950	IL-6	P05231	Fas	P25445	MIF	P14174	MMP 3	P08254
BDNF	P23560	MCP-1	P13500	FGF-9	P31371	sTNFRI	P19438	IP-10	P02778
BMP4	P12644	M-CSF	P09603	GRO alpha	P09341	TIMP-1	P01033	L Selectin	P14151
Eotaxin1	P51671	PDGF BB	P01127	ICAM-1	P05362	TIMP-2	P16035	MMP 1	P03956
GCP-2	P80162	TGF beta1	P01137	IGFBP3	P17936	uPAR	Q03405	PDGF AA	P04085
IGFBP 2	P18065	TNF beta	P01374	IGFBP6	P24592	VEGF	P15692	TIMP-4	Q99727
IL-1ra	P18510	Axl	P30530	IL-8	P10145	ALCAM	Q13740	VEGF R3	P35916

D

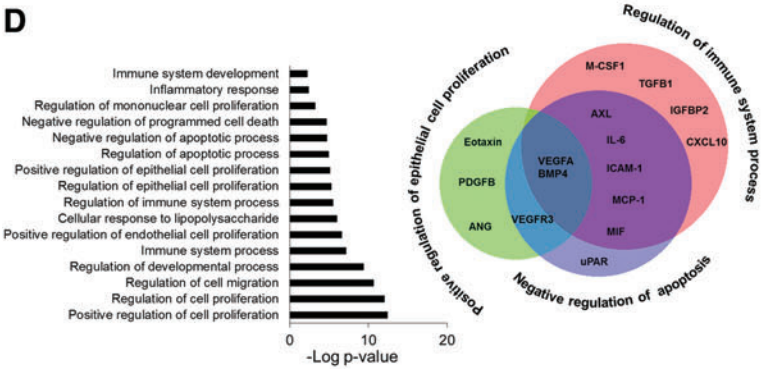

E

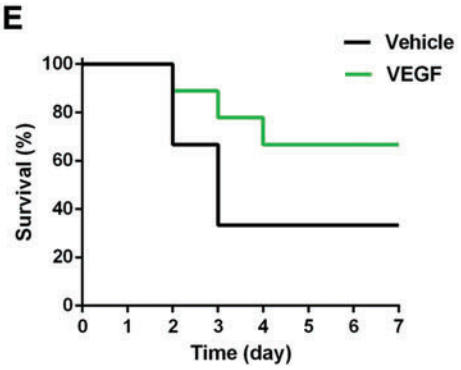

Conclusion

In summary, this report shows that human ESC-MSCs-derived secreted molecules have therapeutic potential for the treatment of an inflammatory hepatic condition. This potentially creates new avenues for the treatment of ALF. Although a variable range of mediators are suggested to be involved in the therapeutic mechanism for ALF, the identification of highly effective molecules or their combinations as therapeutic candidates remains to be elucidated.

Acknowledgments

This study was funded by grants provided from Pasteur Institute of Iran to M.K., and Royan Institute, the Iranian Council of Stem Cell Research and Technology, the Iran National Science Foundation (INSF), Iran Science Elite Federation, and Pasteur Institute of Iran to H.B. The authors express their appreciation to all members of the Liver Program at Royan Institute for their helpful deliberation and consultation during this work. The authors express their appreciation to Zahra Feizi and Zahra Azhdari for their assistance during immunostaining and hepatocyte isolation.

Author Disclosure Statement

No competing financial interests exist.

References

1. Dhaliwal HS and P Singh. (2014). Acute liver failure. N Engl J Med 370:1170.
2. Miwa S, Y Hashikura, A Mita, T Kubota, H Chisuwa, Y Nakazawa, T Ikegami, M Terada, S Miyagawa and S Kawasaki. (1999). Living-related liver transplantation for patients with fulminant and subfulminant hepatic failure. Hepatology 30:1521–1526.
3. Irfan A and I Ahmed. (2015). Could stem cell therapy be the cure in liver cirrhosis? J Clin Exp Hepatol 5:142–146.
4. Owen A and PN Newsome. (2015). Mesenchymal stromal cell therapy in liver disease: opportunities and lessons to be learnt? Am J Physiol Gastrointest Liver Physiol 309:G791–G800.
5. Keating A. (2012). Mesenchymal stromal cells: new directions. Cell Stem Cell 10:709–716.
6. Liu Z, F Meng, C Li, X Zhou, X Zeng, Y He, RJ Mrsny, M Liu, X Hu, JF Hu and T Li. (2014). Human umbilical cord mesenchymal stromal cells rescue mice from acetaminophen-induced acute liver failure. Cytotherapy 16:1207–1219.
7. Christ B, S Bruckner and S Winkler. (2015). The therapeutic promise of mesenchymal stem cells for liver restoration. Trends Mol Med 21:673–686.
8. van Poll D, B Parekkadan, CH Cho, F Berthiaume, Y Nahmias, AW Tilles and ML Yarmush. (2008). Mesenchymal stem cell-derived molecules directly modulate hepatocellular death and regeneration in vitro and in vivo. Hepatology 47:1634–1643.
9. Parekkadan B, D van Poll, K Suganuma, EA Carter, F Berthiaume, AW Tilles and ML Yarmush. (2007). Mesenchymal stem cell-derived molecules reverse fulminant hepatic failure. PLoS One 2:e941.
10. Gadkari R, L Zhao, T Teklemariam and BM Hantash. (2014). Human embryonic stem cell derived-mesenchymal stem cells: an alternative mesenchymal stem cell source for regenerative medicine therapy. Regen Med 9:453–465.
11. Sanchez L, I Gutierrez-Aranda, G Ligero, R Rubio, M Munoz-Lopez, JL Garcia-Perez, V Ramos, PJ Real, C Bueno, et al. (2011). Enrichment of human ESC-derived multipotent mesenchymal stem cells with immunosuppressive and anti-inflammatory properties capable to protect against experimental inflammatory bowel disease. Stem Cells 29:251–262.
12. Ferrer L, EA Kimbrel, A Lam, EB Falk, C Zewe, T Juopperi, R Lanza and A Hoffman. (2016). Treatment of perianal fistulas with human embryonic stem cell-derived mesenchymal stem cells: a canine model of human fistulizing Crohn's disease. Regen Med 11:33–43.
13. Wang X, EA Kimbrel, K Ijichi, D Paul, AS Lazorchak, J Chu, NA Kouris, GJ Yavanian, SJ Lu, et al. (2014). Human ESC-derived MSCs outperform bone marrow MSCs in the treatment of an EAE model of multiple sclerosis. Stem Cell Reports 3:115–130.
14. Baharvand H, SK Ashtiani, A Taee, M Massumi, MR Valojerdi, PE Yazdi, SZ Moradi and A Farrokhi. (2006). Generation of new human embryonic stem cell lines with diploid and triploid karyotypes. Dev Growth Differ 48: 117–128.
15. Hwang NS, S Varghese, HJ Lee, Z Zhang, Z Ye, J Bae, L Cheng and J Elisseeff. (2008). In vivo commitment and functional tissue regeneration using human embryonic stem cell-derived mesenchymal cells. Proc Natl Acad Sci U S A 105:20641–20646.
16. Mohamadnejad M, K Alimoghaddam, M Mohyeddin-Bonab, M Bagheri, M Bashtar, H Ghanaati, H Baharvand, A Ghavamzadeh and R Malekzadeh. (2007). Phase 1 trial of autologous bone marrow mesenchymal stem cell transplantation in patients with decompensated liver cirrhosis. Arch Iran Med 10:459–466.
17. Olivier EN, AC Rybicki and EE Bouhassira. (2006). Differentiation of human embryonic stem cells into bipotent mesenchymal stem cells. Stem Cells 24:1914–1922.
18. Shen L, A Hillebrand, DQ Wang and M Liu. (2012). Isolation and primary culture of rat hepatic cells. J Vis Exp pii: 3917.
19. Jiao J, JM Milwid, ML Yarmush and B Parekkadan. (2011). A mesenchymal stem cell potency assay. Methods Mol Biol 677:221–231.
20. Tahamtani Y, M Azarnia, A Farrokhi, A Sharifi-Zarchi, N Aghdami and H Baharvand. (2013). Treatment of human embryonic stem cells with different combinations of priming and inducing factors toward definitive endoderm. Stem Cells Dev 22:1419–1432.
21. Ishak K, A Baptista, L Bianchi, F Callea, J De Groote, F Gudat, H Denk, V Desmet, G Korb, et al. (1995). Histological grading and staging of chronic hepatitis. J Hepatol 22:696–699.
22. Schnabel LV, CM Abratte, JC Schimenti, MJ Felippe, JM Cassano, TL Southard, JA Cross and LA Fortier. (2014). Induced pluripotent stem cells have similar immunogenic and more potent immunomodulatory properties compared with bone marrow-derived stromal cells in vitro. Regen Med 9:621–635.
23. Milwid JM, JS Elman, M Li, K Shen, A Manrai, A Gabow, J Yarmush, Y Jiao, A Fletcher, et al. (2014). Enriched protein screening of human bone marrow mesenchymal stromal cell secretions reveals MFAP5 and PENK as novel IL-10 modulators. Mol Ther 22:999–1007.
24. Takada Y, T Hisamatsu, N Kamada, MT Kitazume, H Honda, Y Oshima, R Saito, T Takayama, T Kobayashi,

et al. (2010). Monocyte chemoattractant protein-1 contributes to gut homeostasis and intestinal inflammation by composition of IL-10-producing regulatory macrophage subset. J Immunol 184:2671–2676.
25. Hettmer S, L Dannecker, J Foell, MW Elmlinger and GE Dannecker. (2005). Effects of insulin-like growth factors and insulin-like growth factor binding protein-2 on the in vitro proliferation of peripheral blood mononuclear cells. Hum Immunol 66:95–103.
26. Do N, R Zhao, K Ray, K Ho, M Dib, X Ren, P Kuzontkoski, E Terwilliger and SJ Karp. (2012). BMP4 is a novel paracrine inhibitor of liver regeneration. Am J Physiol Gastrointest Liver Physiol 303:G1220–G1227.
27. Fan J, H Shen, Y Sun, P Li, F Burczynski, M Namaka and Y Gong. (2006). Bone morphogenetic protein 4 mediates bile duct ligation induced liver fibrosis through activation of Smad1 and ERK1/2 in rat hepatic stellate cells. J Cell Physiol 207:499–505.
28. Tsugawa D, Y Oya, R Masuzaki, K Ray, DW Engers, M Dib, N Do, K Kuramitsu, K Ho, et al. (2014). Specific activin receptor-like kinase 3 inhibitors enhance liver regeneration. J Pharmacol Exp Ther 351:549–558.
29. Johnson BF, TM Clay, AC Hobeika, HK Lyerly and MA Morse. (2007). Vascular endothelial growth factor and immunosuppression in cancer: current knowledge and potential for new therapy. Expert Opin Biol Ther 7:449–460.
30. Chen L, Y Xu, J Zhao, Z Zhang, R Yang, J Xie, X Liu and S Qi. (2014). Conditioned medium from hypoxic bone marrow-derived mesenchymal stem cells enhances wound healing in mice. PLoS One 9:e96161.
31. Banas A, T Teratani, Y Yamamoto, M Tokuhara, F Takeshita, M Osaki, M Kawamata, T Kato, H Okochi and T Ochiya. (2008). IFATS collection: in vivo therapeutic potential of human adipose tissue mesenchymal stem cells after transplantation into mice with liver injury. Stem Cells 26:2705–2712.
32. Zagoura DS, MG Roubelakis, V Bitsika, O Trohatou, KI Pappa, A Kapelouzou, A Antsaklis and NP Anagnou. (2012). Therapeutic potential of a distinct population of human amniotic fluid mesenchymal stem cells and their secreted molecules in mice with acute hepatic failure. Gut 61:894–906.

Address correspondence to:
Dr. Hossein Baharvand
Department of Stem Cells and Developmental Biology
Cell Science Research Center
Royan Institute for Stem Cell Biology and Technology
ACECR
Tehran 1665659911
Iran

E-mail: baharvand@royaninstitute.org

Mehdi Kadivar
Biochemistry Department
Pasteur Institute of Iran
Tehran 13164
Iran

E-mail: kadivar@pasteur.ac.ir

Received for publication August 6, 2016
Accepted after revision September 23, 2016
Prepublished on Liebert Instant Online September 27, 2016